

# Sensitivity dependence with respect to diaphragm dimensions in a glass-based integrated optic pressure sensor

Yoshihiko Iwase<sup>a</sup>, Yumi Okamoto<sup>a</sup>, Masashi Ohkawa<sup>\*b</sup>, Seishi Sekine<sup>b</sup>, and Takashi Sato<sup>b</sup>

<sup>a</sup>Niigata University, Graduate School of Science and Technology, Ohkawa Lab.  
8050 Ikarashi 2-no-cho, Niigata 950-2181, Japan

<sup>b</sup>Niigata University, Faculty of Engineering  
8050 Ikarashi 2-no-cho, Niigata 950-2181, Japan

## ABSTRACT

In this paper, the relationship between sensitivity and diaphragm dimensions in a glass-based integrated optic pressure sensor is described. The sensor has a rectangular diaphragm as a pressure-sensitive structure and a straight sensing waveguide across the diaphragm. The sensor operation is based on the phenomenon that a phase difference between two orthogonal guided modes is induced by the elasto-optic effect in the presence of applied pressure. The sensitivity of the sensor is theoretically known to be dependent on the thickness and side length of the diaphragm. Such dependencies are worth investigating to obtain helpful design rules for miniaturization of the sensor, but have not been examined experimentally in detail. In this study, to examine the relationship between sensitivity and thickness, two sensors were fabricated with 10 mm × 10 mm × 0.3 mm (sensor #1) and 10 mm × 10 mm × 0.22 mm (sensor #2) diaphragms. The sensitivity of sensor #2 was larger than that of sensor #1 by a factor of 1.72, which closely agreed with the theoretical factor of 1.86. Moreover, to determine the relationship between sensitivity and side length, two more sensors, besides sensor #2, with 7mm-square (sensor #3) and 14mm-square (sensor #4) diaphragms were fabricated with a diaphragm thickness of 0.22 mm. The measured sensitivities agreed approximately with the theoretical ones although there was a slight difference in sensor #4.

**Keywords:** integrated optics, pressure sensor, elasto-optic effect, glass, diaphragm

## 1. INTRODUCTION

Since the late 1980's, several groups have demonstrated integrated optic pressure sensors with micro-machined diaphragms.<sup>1-5</sup> Our group has been also developing glass-based and silicon-based integrated optic pressure sensors using intermodal interference between the fundamental TM-like and TE-like modes.<sup>6-10</sup> These sensors have excellent features for medical applications, *e.g.* immunity to electromagnetic interference and the impossibility of an electric spark. One of our targets for medical application is to realize an integrated optic pressure sensor, which can be incorporated into a catheter for measuring blood pressure measurement. In realization of a miniaturized sensor, it is worthwhile to investigate the relationship between sensitivity and diaphragm dimensions. The sensitivity of the sensor is theoretically known to be inversely proportional to the square of the thickness of the diaphragm.<sup>6</sup> In addition, according to the theoretical prediction, the sensitivity is proportional to the cube of either side length of the diaphragm.<sup>6</sup> Therefore, when the area of the diaphragm is reduced for the miniaturization, the thickness must be concurrently thinned to maintain the sensitivity. Such theoretical predictions have yet to be confirmed experimentally. In this study, to reveal dependence on the thickness, two sensors with 0.22mm-thick and 0.3mm-thick diaphragms were fabricated using glass substrates, the area of the diaphragm remaining constant at 10 mm × 10 mm. Regarding the dependence on the side length, two more glass-based sensors with 7mm-square and 14mm-square diaphragms were built with a diaphragm thickness of 0.22 mm. The measured sensitivities versus the thickness and side length almost agreed with the theoretical estimates. Incidentally, in this study, glass was utilized as a substrate although silicon is the more suitable substrate for miniaturizing the sensors with micro-mechanical structures. For a reliable comparison between the theoretical and experimental results, glass is an excellent substrate because of its well-known mechanical and optical parameters. The findings obtained in this study could be applied in designing the silicon-based integrated optic pressure sensors for miniaturization although proper modifications would be required.

## 2. PRINCIPLE OF SENSOR OPERATION

Figure 1 shows the integrated optic pressure sensor using intermodal interference between the fundamental TM-like and TE-like modes. The sensor has a rectangular diaphragm as a pressure-sensitive mechanical structure and a straight single-mode waveguide over the diaphragm. The diaphragm is distorted when a pressure difference is applied to the diaphragm. The distortion causes strain, which produces a change in the refractive index of the diaphragm by the elasto-optic effect. The index change yields phase retardation in the lightwave, which propagates in the waveguide on the diaphragm. Since the phase retardation is generally dependent on the guided modes, the phase difference between the two modes is also a function of the applied pressure. To detect the phase difference, the sensor is placed in a pair of crossed polarizers as shown in Fig. 2. The input polarizer is oriented at  $45^\circ$  with respect to the polarization of each guided mode. The light beam through the input polarizer is coupled to the TM-like and TE-like modes at equal intensities. At the end of the waveguide, the lightwave has linear, elliptic or circular polarization, corresponding to the induced phase difference between the two guided modes. The crossed output polarizer converts the polarization-modulated light into intensity-modulated light. The intensity of the light beam passing through the output polarizer sinusoidally changes with the applied pressure. Therefore, the pressure applied to the diaphragm can be determined from the output intensity.

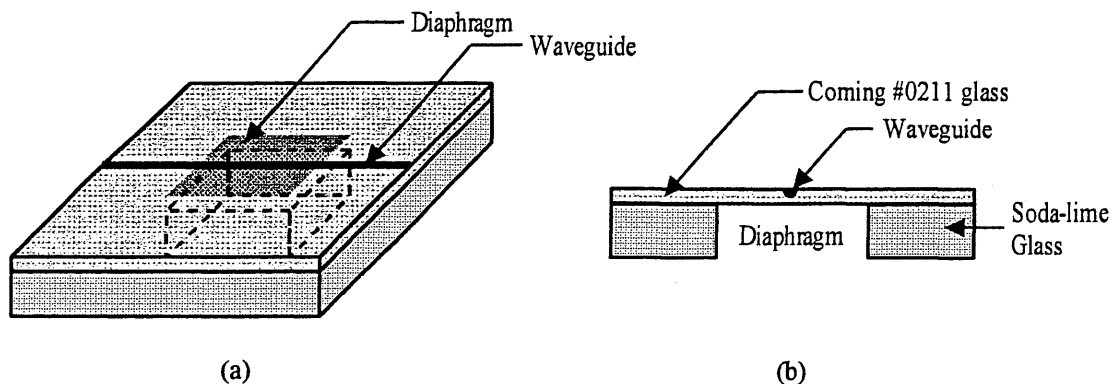


Fig. 1 (a) Schematic drawing of the integrated optic pressure sensor using intermodal interference, and (b) its cross-sectional view.

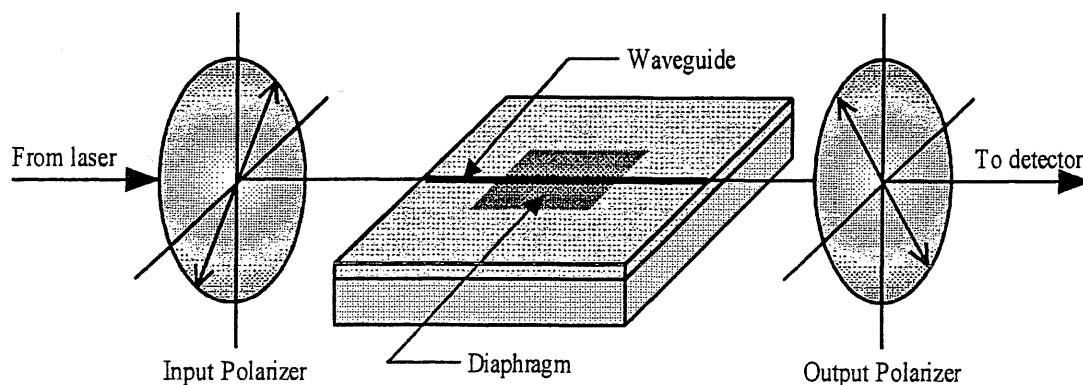


Fig. 2 The sensor placed between a pair of crossed polarizers to convert the phase difference between the two guided modes into the change in the light intensity.

### 3. THEORETICAL RESULTS

#### 3.1 Phase sensitivity versus waveguide position

Sensitivity is more dependent on the position of the sensing waveguide than on the diaphragm dimensions because the index change due to the applied pressure is not uniformly distributed across the diaphragm.<sup>8-10</sup> To avoid being influenced by the waveguide position, it is important to understand the relationship between sensitivity and waveguide position. So, the phase difference per unit pressure, that is, the phase sensitivity, was calculated as a function of the waveguide position, following the mathematical description in Ref. 10. In the calculation, a rectangular diaphragm with an area of  $a \times b$  and a thickness of  $t$  was assumed. It was also assumed that the waveguide was placed parallel to side  $b$  and the pressure was uniformly applied over the diaphragm with all edges rigidly clamped. The theoretical calculation was carried out using the optical and mechanical parameters of the Corning #0211 glass, but the elasto-optic coefficients of silica were used instead of those of the Corning glass. Figure 3 shows the calculated sensitivity versus the waveguide position for the square diaphragm. The phase sensitivities are normalized to be at unity at  $y = \pm a/2$ . The phase sensitivity has a maximum value when the waveguide is located along the diaphragm edge, but the sensitivity rapidly decreases as the waveguide deviates from the edge. When the waveguide is located at the center of the diaphragm, the sensitivity hardly decreases even if the waveguide deviates from the center. Therefore, the center of the diaphragm was chosen as the waveguide position to compare the sensitivity in varying diaphragm dimensions in this study.

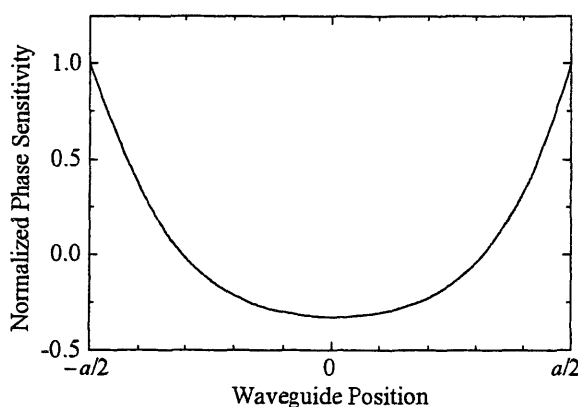


Fig.3 Normalized phase sensitivity as a function of waveguide position.

#### 3.2 Phase sensitivity versus thickness of diaphragm

Figure 4 shows the calculated sensitivity as a function of the thickness of the diaphragm. In the calculation, the waveguide was assumed to be at the center of the diaphragm, where sensitivity is minimally affected by the deviation of the waveguide position as described above. The wavelength of the guided light was set to be 633 nm, and the side length of the square diaphragm was 10 mm. From the figure, since the slope is  $-2$  in log-log graph, the sensitivity is inversely proportional to the square of the diaphragm thickness. Such relationship between sensitivity and thickness holds for any rectangular diaphragm.

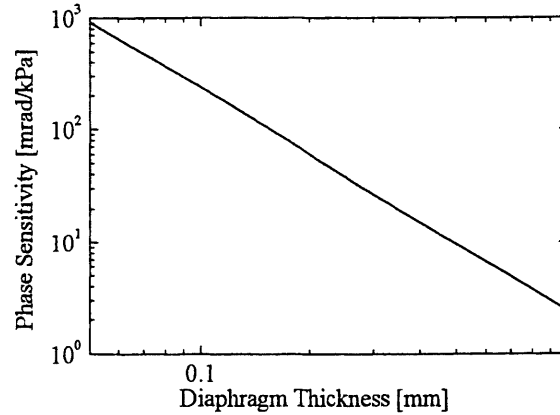


Fig. 4 Phase sensitivity as a function of thickness of diaphragm.

### 3.3 Phase sensitivity versus side length of diaphragm

Figure 5 shows the calculated phase sensitivity as a function of the side length of the square diaphragm. The diaphragm thickness and wavelength were set to be 0.22 mm and 633 nm, respectively. It was assumed that the waveguide position was located along the center of the diaphragm. It is found from the figure that the slope is 3 in log-log graph. Therefore, the sensitivity is proportional to the cube of the side length, or to the three-halves power of the area. This relationship is valid for any rectangular diaphragm if the side length ratio remains constant while changing the side lengths.

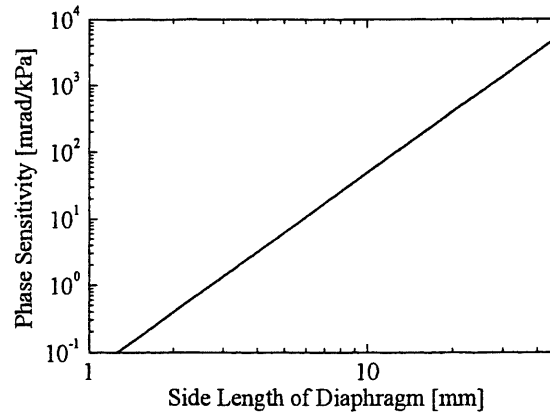


Fig.5 Phase sensitivity as a function of side length of diaphragm.

## 4. EXPERIMENT

### 4.1 Fabrication and measurement

The sensors were built using two glasses: a Corning #0211 glass as a diaphragm plate and a soda-lime glass with a square hole to support the diaphragm plate. First, a thin aluminum film was evaporated on a Corning glass. The aluminum film was removed by using a patterned photoresist as a mask. Then, the glass was immersed  $\text{KNO}_3$  for two hours at  $400^\circ\text{C}$  to form single-mode channel waveguides. Before the two substrates were joined, the waveguide was adjusted to be parallel to the diaphragm. Finally, both substrates were bonded together by UV adhesion. The diaphragm dimensions of the fabricated sensors were chosen to be  $10\text{ mm} \times 10\text{ mm} \times 0.3\text{ mm}$  (sensor #1) and  $10\text{ mm} \times 10\text{ mm} \times 0.22\text{ mm}$  (sensor #2) to

examine the relationship between sensitivity and thickness. Moreover, besides sensor #2, two more sensors with 7mm-square (sensor #3), and 14mm-square (sensor #4) diaphragms were fabricated with a diaphragm thickness of 0.22 mm to determine the relationship between sensitivity and side length.

Figure 6 shows the experimental setup to measure the output intensity versus the applied pressure. The sensitivity was measured using a linearly-polarized He-Ne laser at 633 nm. The polarization of the laser beam was set at  $45^\circ$  to the sensor surface, so that an input polarizer shown in Fig. 2 was not necessary. The sensor was connected to a syringe by a silicone tube in order to apply pressure to the diaphragm. Pulling and pushing on the plunger of the syringe caused the pressure difference, ranging from  $-40$  kPa to  $60$  kPa, on the diaphragm. A positive value represents that the pressure on the bottom side of the diaphragm plate is higher than that of the atmosphere.

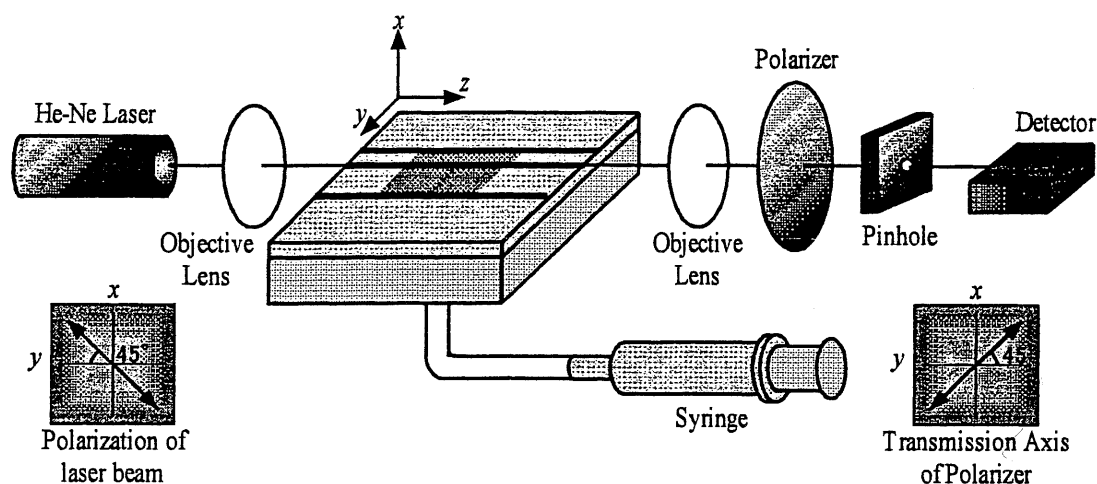


Fig. 6 Experimental setup to measure the output intensity as a function of the applied pressure.

#### 4.2 Experimental results with respect to diaphragm thickness

Figure 7 shows the experimental results of sensor #1 with a 0.3mm-thick diaphragm for the waveguide nearest to the center of the diaphragm. Also, Fig. 8 shows the results of sensor #2 with a 0.22mm-thick diaphragm. The solid line in each figure

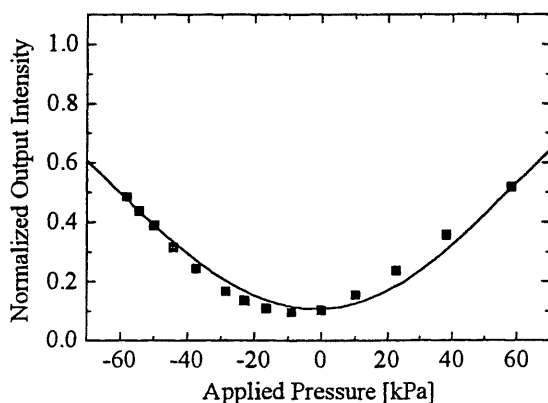


Fig. 7 Normalized output intensity versus applied pressure for the waveguide nearest to the center of the diaphragm of sensor #1 with a 0.3mm-thick diaphragm.

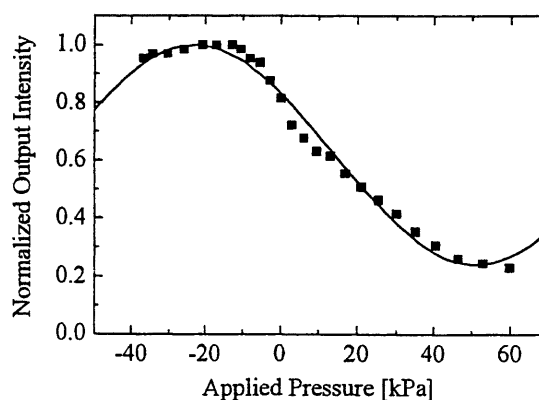


Fig. 8 Normalized output intensity versus applied pressure for the waveguide nearest to the center of the diaphragm of sensor #2 with a 0.22mm-thick diaphragm.

indicates the computer projection of the experimental data. A half period of the output intensity is called the halfwave pressure, which corresponds to a phase difference of  $\pi$  rad. The phase sensitivity is defined as the phase difference between the two guided modes per unit pressure. From Figs. 7 and 8, the halfwave pressure is evaluated to be 127 kPa and 74.0 kPa, corresponding to phase sensitivities of 24.7 mrad/kPa and 42.5 mrad/kPa, respectively. Figure 9 shows the calculated and measured sensitivities as a function of diaphragm thickness. Also, Table 1 indicates the calculated and measured values of the two sensors. From Table 1, the measured sensitivities are about 90% of the theoretical sensitivity. The measured sensitivity of sensor #2 was higher than that of sensor #1 by a factor of 1.72, which closely agreed with the theoretical factor of 1.86. Therefore, it is found theoretically and experimentally that the sensitivity is inversely proportional to the square of the diaphragm thickness although further experimental results are necessary for a detailed comparison between the theoretical and experimental results.

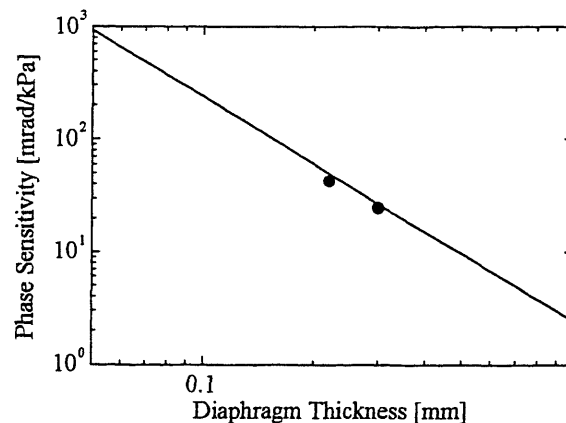


Fig. 9 Measured sensitivities of sensors #1 and #2 are shown as dots. The solid line indicates the calculated sensitivities as a function of diaphragm thickness.

Table 1 The calculated and measured sensitivities of sensors #1 and #2 for comparison in regards to the dependence on the thickness

Sensor #	Diaphragm Dimensions [mm $\times$ mm $\times$ mm]	Calculated [mrad/kPa]	Measured [mrad/kPa]
1	10 $\times$ 10 $\times$ 0.3	26.9	24.7
2	10 $\times$ 10 $\times$ 0.22	49.9	42.4

#### 4.3 Experimental results with respect to side length of diaphragm

Figure 10 shows the experimental results of sensor #3 with a 7mm-square diaphragm for the waveguide nearest to the center of the diaphragm. Also, Fig. 11 shows the result of sensor #4 with a 14mm-square diaphragm. From Figs. 10 and 11, the halfwave pressure is evaluated to be 203 kPa and 35.0 kPa, corresponding to a phase sensitivity of 15.5 mrad/kPa and 89.7 mrad/kPa, respectively. Figure 12 shows the calculated and measured sensitivities versus side length of the diaphragm. The measured sensitivities are almost on the theoretical line, but there is a slight deviation in sensor #4. Table 2 shows the calculated and measured values of the three sensors. From Table 2, the measured sensitivities of sensors #2 and #3 are about 90% of the theoretical sensitivities, while that of sensor #4 is only 65%. In comparing sensors #2 and #4, the measured sensitivity of sensor #4 was higher than that of sensor #2 by a factor of 2.11, which is 77% of the theoretical factor. Although the slight difference exists in sensor #4, it still has been found theoretically and experimentally that the sensitivity is proportional to the cube of the side length of the diaphragm.

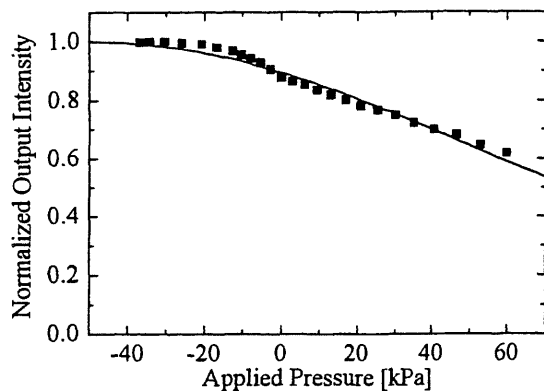


Fig. 10 Normalized output intensity versus applied pressure for the waveguide nearest to the center of the diaphragm in sensor #3 with a 7mm-square diaphragm.

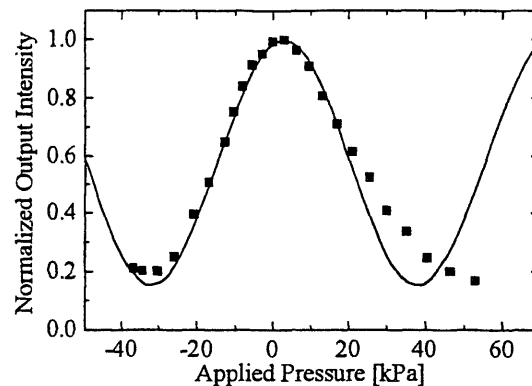


Fig. 11 Normalized output intensity versus applied pressure for the waveguide nearest to the center of the diaphragm in sensor #4 with a 14mm-square diaphragm.

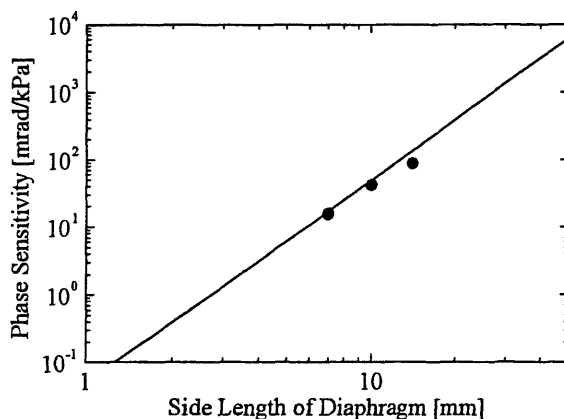


Fig. 12 Measured sensitivities of sensors #2, #3 and #4 are shown as dots. The solid line indicates the calculated sensitivities as a function of side length.

Table 2 The calculated and measured sensitivities of sensors #2, #3 and #4 for comparison in regards to the dependence on side length.

Sensor #	Diaphragm Dimensions [mm×mm×mm]	Calculated [mrad/kPa]	Measured [mrad/kPa]
3	7 × 7 × 0.22	17.1	15.5
2	10 × 10 × 0.22	49.9	42.4
4	14 × 14 × 0.22	136	89.7

## 5. CONCLUSIONS

We experimentally examined the relationship between sensitivity and diaphragm dimensions in the glass-based integrated optic pressure sensor. Regarding the dependence on thickness, it was proven from the calculated and measured results that sensitivity is inversely proportional to thickness. Also, regarding the dependence on side length, sensitivity was found to be

proportional to the cube of the side length theoretically and experimentally. From these dependencies, a scale-reduction rule accompanied by no sensitivity drop can be derived. The rule is that the sensitivity is constant even if the dimensions of the rectangular diaphragm are reduced as long as both the side length ratio  $a/b$  and the characteristic length  $a^3/t^2$  remain constant. Here, the characteristic length is defined as the ratio of the cube of either side length and the square of the thickness. Such a scale-reduction rule can be applied to silicon-based integrated optic sensors, and is very helpful in designing miniaturized sensors.

## 6. ACKNOWLEDGEMENT

This work is, in part, supported by a Grant-in-Aid for Scientific Research (No.12650339) from the Japan Society for the Promotion of Science.

## REFERENCES

1. M. Tabib-Azar, and G. Beheim, "Modern trends in microstructures and integrated optics for communication, sensing, and actuation," *Opt. Eng.*, **36**, pp.1307-1318, 1997.
2. M. Ohkawa, M. Izutsu, and T. Sueta, "Integrated optic pressure sensor on silicon substrate," *Appl. Opt.*, **28**, pp.5153-5157, 1989.
3. G. N. De Brabander, J. T. Boyd, and G. Beheim, "Integrated optical ring resonator with micromechanical diaphragm for pressure sensing," *IEEE Photon. Technol. Lett.*, **6**, pp.671-673, 1994.
4. G. N. De Brabander, Glenn Beheim, and J. T. Boyd, "Integrated optical micromachined pressure sensor with spectrally encoded output and temperature compensation," *Appl. Opt.*, **37**, pp.3264-3267, 1998.
5. H. Porte, V. Gorel, S. Kiryenko, J. Goedgebuer, W. Daniau, and P. Blind, "Imbalanced Mach-Zehnder interferometer integrated in micromachined silicon substrate for pressure sensor," *J. Lightwave Technol.*, **17**, pp.229-233, 1999.
6. M. Ohkawa, K. Hasebe, C. Nishiwaki, S. Sekine, and T. Sato, "Integrated optical pressure sensor using intermodal interference between two mutual orthogonal guided-modes," *Optical Review*, **7**, pp.144-148, 2000.
7. M. Ohkawa, C. Nishiwaki, K. Hasebe, S. Sekine, and T. Sato, "Glass-Based Integrated Optic Pressure Sensors with a Mach-Zehnder Interferometer and with an Intermodal Interferometer," *Proc. SPIE*, **3936**, pp.309-318, 2000.
8. T. Goto, A. Yamada, M. Ohkawa, S. Sekine, and T. Sato, "An Experimental Investigation of Sensitivity Dependence with respect to Waveguide Position on a Micromachined Diaphragm in a Silicon-Based Integrated Optic Pressure Sensor," *Proc. SPIE*, **4591**, pp.337-344, 2001.
9. M. Ohkawa, Y. Shirai, T. Goto, S. Sekine, and T. Sato, "Silicon-Based Integrated Optic Pressure Sensor Using Intermodal Interference between TM-Like and TE-Like Modes," *Fiber and Integrated Optics*, **21**, pp.105-113, 2002.
10. M. Ohkawa, K. Hasebe, S. Sekine, and T. Sato, "Relationship between Sensitivity and Waveguide Position on the Diaphragm in Integrated Optic Pressure Sensors Based on the Elasto-Optic Effect," *Appl. Opt.*, **41**, pp.5016-5021, 2002.

\*Correspondence: E-mail: [ohkawa@eng.niigata-u.ac.jp](mailto:ohkawa@eng.niigata-u.ac.jp); Telephone & Fax: +81-25-262-6734